1980AJ.....85..499P

HIGH-RESOLUTION OBSERVATIONS OF 3C219 AT 1.48 AND 4.89 GHz

R. A. PERLEY
National Radio Astronomy Observatory, [a] VLA Program, Socorro, New Mexico 87801

A. H. BRIDLE
Queen's University at Kingston, Ontario K7L 3N6, Canada

A. G. WILLIS
Netherlands Foundation for Radio Astronomy, Radiosterrenwacht Westerbork, The Netherlands

E. B. FOMALONT
National Radio Astronomy Observatory, [a] Charlottesville, Virginia 22901
Received 15 October 1979; revised 4 February 1980

ABSTRACT

The VLA has been used to make high-resolution maps of the double radio galaxy 3C219 at 1.48 and 4.89 GHz. The radio jet in 3C219 contains two main components, each of which is composed of two or more subcomponents. The jet is highly polarized with the magnetic field oriented along its length, and its width decreases with increasing distance from the nucleus. In both of these characteristics, the jet in 3C219 differs appreciably from the jets in low-luminosity radio galaxies recently mapped at the VLA. The two distant lobes of 3C219 both contain compact structure. In the south-preceding lobe, this structure is L-shaped, while in the north-following lobe it is a nearly complete circular ring. The degree of linear polarization is high throughout both lobes, both in the compact structures and in the diffuse regions which surround them. The magnetic field configuration in the northern lobe is circumferential, both in the diffuse region and in the compact ring.

I. INTRODUCTION

The radio source 3C219 is identified with a $17^{m}.5$ cD1 galaxy with a redshift $z = 0.1745$ (Schmidt 1965) and is the brightest member of a compact Zwicky cluster (Macdonald *et al.* 1968). Its structure has recently been mapped with moderate resolution and sensitivity at several frequencies between 1 and 10 GHz (Burch 1979a; De Young *et al.* 1979; Högbom 1979). Turland (1975) obtained the first evidence for a narrow radio jet ~80 kpc long within the basically "classical double" structure of 3C219. The jet begins near a small-diameter radio core in the nucleus of the galaxy and extends toward the south-preceding radio lobe. As 3C219 is the most luminous radio galaxy presently known to contain a radio jet, we have included it in a program of VLA observations of galaxies with jets and emission bridges. Results from this program have been presented for NGC 315 by Bridle *et al.* (1979), for 3C449 by Perley *et al.* (1979), and for 3C31 by Fomalont *et al.* (1980); we refer to these, respectively, as Papers I, II, and III in what follows.

This paper reports observations of 3C219 using the VLA at 1.48 GHz (λ20 cm) and 4.89 GHz (λ6 cm), which give new information on the structure in and around the radio jet and which also delineate the morphology of the bright compact structures in the outer lobes of the source.

II. OBSERVATIONS

The observations were taken with 12 antennas of the partially completed VLA on 29 September 1978 for λ6 cm and 30 September 1978 for λ20 cm. Table I lists the main parameters of the observations. The data were calibrated against the nearby source 0917+449, whose flux density was itself calibrated against that of the standard source 1328+307 (=3C286) on the scale of Baars *et al.* (1977).

The configuration of the VLA at the time of these observations could not sample a 30° sector of the (u,v) plane at the declination of 3C219. The maps have been "CLEANED" in the standard manner (Högbom 1974), but because the major axis of the source lies in the unsampled sector, some Fourier components along this axis may not be correctly estimated by the CLEAN algorithm. In addition, the shortest (projected) spacing was 0.25 km (u) by 0.16 km (v), so structure components of scale size $\gtrsim 50'' \times \gtrsim 90''$ at 1480 MHz, and $\gtrsim 15'' \times \gtrsim 30''$ at 4885 MHz will be attenuated in our maps. This

[a] The National Radio Astronomy Observatory is operated by Associated Universities, Inc., under contract with the National Science Foundation.

 0004-6256/80/050499-08$00.90 © 1980 Am. Astron. Soc.

© American Astronomical Society • Provided by the NASA Astrophysics Data System

1980AJ.....85..499P

TABLE I.

Parameters of VLA observations of 3C219

Frequency	Bandwidth	T_{sys} (K)	HA range	Feed polarizations
1480	12 MHz	60	-5^h0 to $+7^h0$	orthogonal linear
4885	50 MHz	50	-4^h7 to $+7^h0$	opposite circular

Position of antennas on 30 September 1978

Azimuth	175°	115°	236°	236°	115°	236°	115°	236°	236°	236°	236°	236°
Distance (km)	0.04	0.48	0.48	0.71	0.97	1.26	1.59	1.59	3.19	5.22	7.66	10.47

Calibration parameters

Source	α(1950.0)	δ(1950.0)	S_{1480} (Jy)	S_{4885} (Jy)
0.917 + 449	$09^h17^m41^s.90$	44°54′39″.8	0.66	0.80

Source scan length: 12[a] min
Calibrator scan length: 3 min

[a] For first $4^h.5$, at 1480 MHz, observations were time shared with another source, resulting in a duty cycle of 1:3 for 3C219.

is a problem only at 4885 MHz, where the size of the source much exceeds this limit.

III. THE LARGE-SCALE STRUCTURE OF 3C219

Figure 1 shows a λ20 cm map of the entire source obtained by tapering our data with a Gaussian function falling to 50% at 8.8 km. The beam is 3.0 arcsec × 5.3 arcsec (FWHM), major axis at p.a. 106°. The line joining the radio core, the high-brightness jet, and the bright knot in the south-preceding lobe is surrounded by diffuse low-brightness emission for the entire distance from the core to the knot. There is also diffuse emission around this line extending ~20 arcsec beyond the knot. The north-following lobe also contains a bright knot surrounded by more diffuse emission; this diffuse emission trails back to form a bridge to the central source. The compact knots in each lobe are not collinear with the radio core; a line from the core to the north-following knot would intersect the line from the core to the south-preceding knot at an angle of ~9°.

The general distribution of the diffuse emission in the southern lobe differs from that of the northern; in the former, the diffuse emission is elongated along the major axis of the source, whereas in the latter it is more rounded. The appearance of compact knots within the diffuse emission is reminiscent of similar features in the giant radio galaxy DA240 (Willis *et al.* 1974).

IV. THE RADIO CORE AND JET

Figure 2 shows a λ6 cm map at 0.85 by 1.2 arcsec resolution (FWHM, major axis at p.a. 147°) of the radio core and the bright jet. The core is unresolved (angular diameter $\lesssim$0.25 arcsec) and has a spectrum typical of a synchrotron self-absorbed source with $\alpha = -0.43 \pm 0.08$ ($S_\nu \propto \nu^{-\alpha}$). Its flux density in our λ6 cm map is 42 ± 4 mJy, while that at λ20 cm is 25 ± 3 mJy. The position of the radio core is $\alpha(1950.0) = 09^h17^m50^s.662 \pm 0^s.015$, $\delta(1950.0) = 45°51'43''.55 \pm 0''.2$.

The jet consists of two major components ~8 arcsec (20 kpc, $H_0 = 75$ km s^{-1} Mpc^{-1}) apart, both of which are themselves composed of two or more subcomponents. The component farther from the core is ~6 arcsec (15 kpc) long, whereas the other component is only 3.5 arcsec (9 kpc) long. There is a well defined gap of ~5 arcsec (13 kpc) between the core and the closest detected part of the jet. Similar gaps occur at the bases of the radio jets in NGC 315 (Paper I), 3C449 (Paper II), and 3C31 (Paper III), but the linear size of the gap in 3C219 is the largest we have yet found. The jet is not straight, but curves southward slightly before its intensity falls off rapidly ~19 arcsec (49 kpc) from the radio core.

The jet is slightly resolved to our λ6 cm beam. Table II gives the deconvolved full widths of the jet at half maximum at five points along the jet. The angle given in column 6 is the cone angle of the jet with the radio core as apex. The width of the jet decreases towards the leading edge of its farther component. The decreasing width of this jet in 3C219 contrasts strongly with the behavior of the jets in NGC 315 (Paper I), 3C449 (Paper II), and 3C31 (Paper III), whose widths generally increase with increasing distance from their radio cores. At our sensitivity there is no evidence of a counter-jet, implying a brightness ratio of >20:1 between the observed jet and any hypothetical counter-jet.

The degree of linear polarization of the jet is very high, averaging 30% and reaching 60% in places. The degree of polarization falls rapidly at the leading edge of the farther component. This could be explained by bending

TABLE II. Jet widths.

Point	Angle from nucleus	Measured jet width	Beam FWHM[a]	Deconvolved jet width	Cone angle
1	6″.7	2″.0 ± .10	1″.47 ± 0.05	1″.35 ± 0.15	11°
2	9″.3	2″.1 ± 0.10	1″.47	1″.50 ± 0.15	9°
3	14″.8	1″.85 ± 0.10	1″.41	1″.20 ± 0.15	5°
4	16″.2	1″.68 ± 0.10	1″.41	0″.91 ± 0.2	3°
5	17″.9	1″.65 ± 0.10	1″.35	0″.95 ± 0.2	3°

[a] At p.a. of measured jet width.

© American Astronomical Society • Provided by the NASA Astrophysics Data System

1980AJ.....85..499P

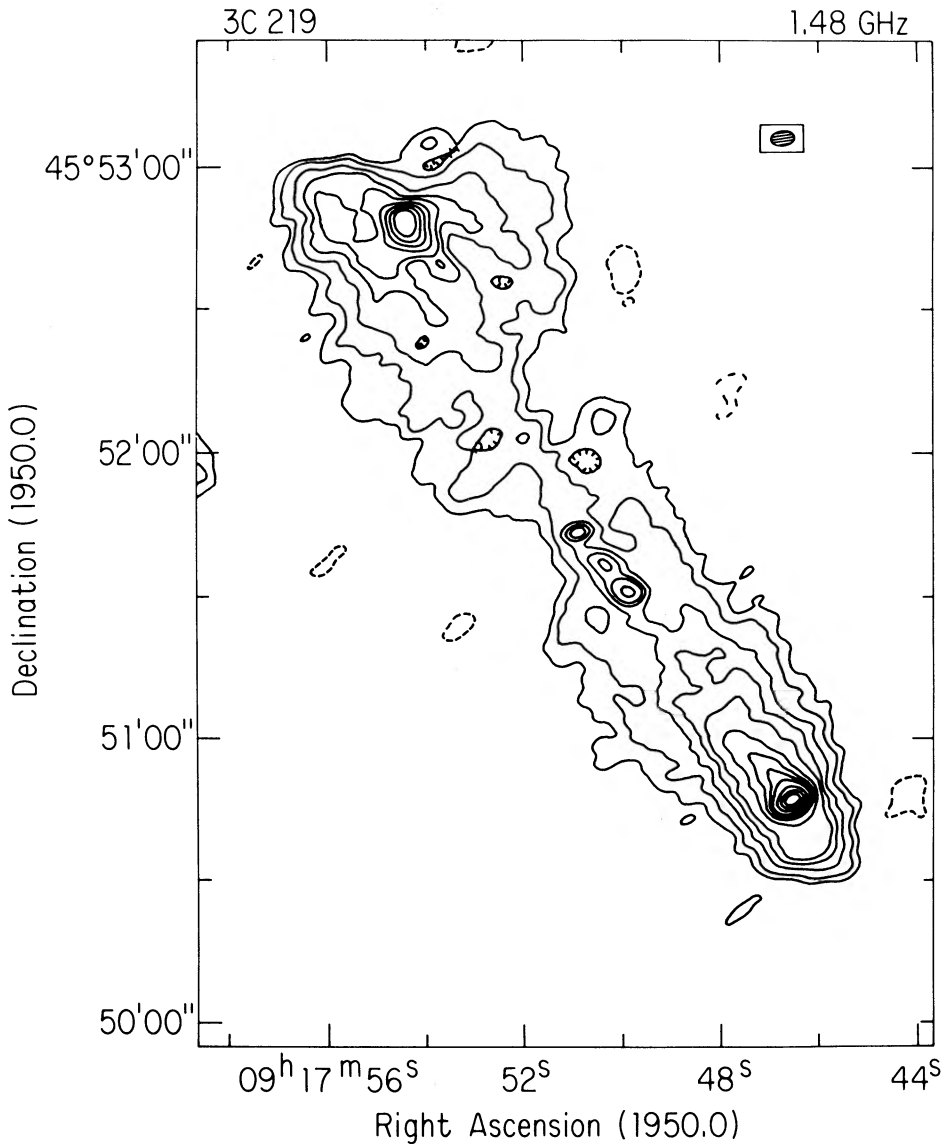

FIG. 1. Contour map of 3C219 at λ20 cm. The contour levels are −5, 5, 10, 20, 30, 40, 60, 80, 100, 120, 160, 200, and 240 mJy/beam. The full width half-power beam (3.0 arcsec × 5.3 arcsec, major axis at p.a. 106°) is shown by the hatched ellipse at upper right.

of the magnetic field around the extremity of the component on an angular scale smaller than our resolution. The value of the integrated rotation measure for 3C219 (Burch 1979a) is −9 rad/m^2 and implies that the correction to intrinsic E-vector orientations is less than 2° at λ6 cm, i.e., the measured polarization position angles are equal to the intrinsic angles to within the measurement errors. As the observed E vectors are nearly perpendicular to the jet axis, the dominant component of the magnetic field in the jet must lie nearly along the jet, confirming the results of Burch (1979a), Högbom (1979), and De Young *et al.* (1979). The scale of this parallel-field region contrasts with those in NGC 315, 3C31, and 3C449, in which such field configurations persist for only a few (<10) kpc from the cores before evolving into perpendicular-field configurations (Papers II and III).

We have applied the minimum energy analyses to our observations using the equations and assumptions given in Paper II. The results are given in Table III. The minimum energy density and total energy content of the jet in 3C219 are respectively about 10 and 40 times that

TABLE III. Equipartition parameters of the jet.[a]

Component	Emissivity (erg s^{-1} cm^{-3} ster^{-1})	B_{min} (μG)	u_{min} (erg cm^{-3})	E_{min}^{total} (erg)
Preceding	8.1×10^{-27}	32	9.7×10^{-11}	4×10^{56}
Following	1.9×10^{-27}	21	4.2×10^{-11}	3×10^{56}

[a] Assuming cylindrical geometry with jet axis and magnetic field perpendicular to the line of sight, spectral index of +0.7 extending from 10 MHz to 10 GHz, and equal energies in relativistic electrons and protons.

© American Astronomical Society • Provided by the NASA Astrophysics Data System

1980AJ.....85..499P

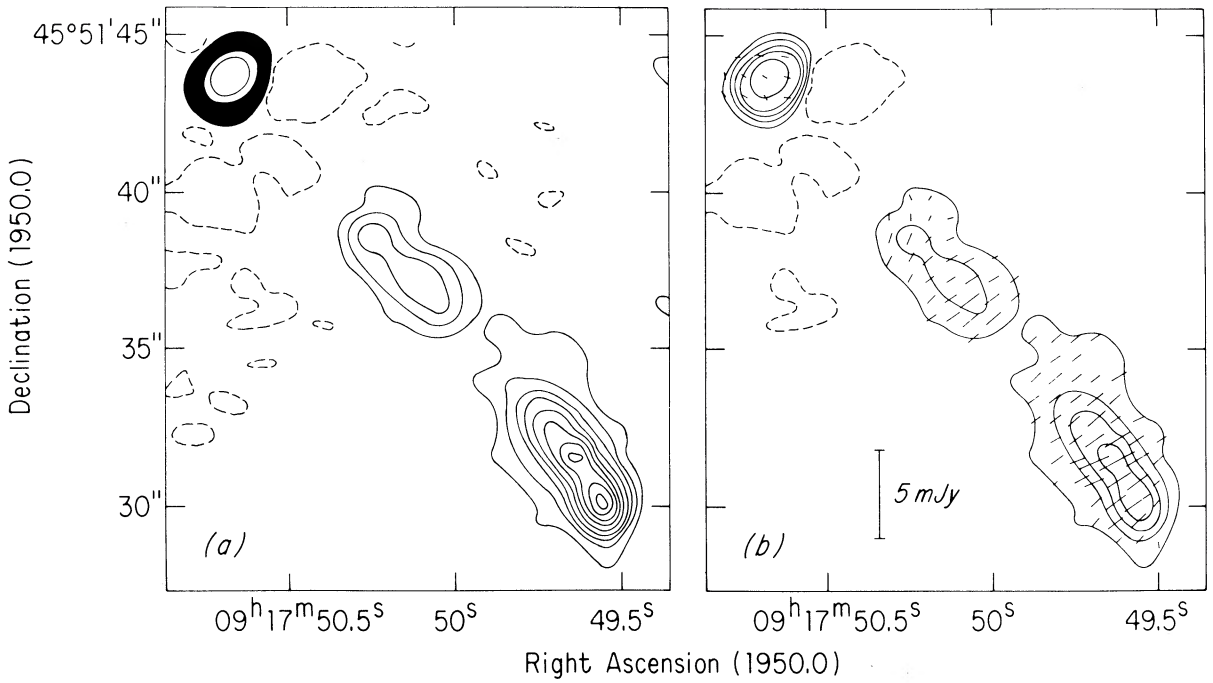

FIG. 2. (a) Contour map of total intensity in the radio core and in the jet of 3C219 at λ6 cm. The contour levels are −0.8, 0.8, 1.6, 2.4, 3.2, 4.0, 4.8, 5.6, 6.4, 7.2, 9.9, and 19.8 mJy/beam. The full width half-power beam (0.85 arcsec × 1.2 arcsec, major axis at p.a. 147°) is indicated by the thin contour around the peak of the bright radio core. (b) The distribution of the linear polarization over the radio core and jet of 3C219 at λ6 cm. The lengths of the line segments indicate the polarized intensities, and their orientations indicate the position angles of the *E* vectors. Resolution is as in (a).

of the jet in 3C449 (Paper II). Although the absolute values of the energy parameters depend on the assumptions made in the equipartition calculations (e.g., electron-to-proton energy ratio), the relative values in the two sources are less likely to be sensitive to the particular assumptions made.

De Young *et al.* (1979) claimed to have detected an increase in the spectral index of the jet with increasing distance from the core, based on their observations at 2.7 and 8.1 GHz. Our data (Table IV) show that the spectral indices of the two main components of the jet emission between 1.48 and 4.89 GHz are not significantly different, and thus do not confirm this result. The discrepancy is probably caused by contamination of the jet by the extended, underlying emission at the resolution used by De Young *et al.* (1979).

A weak argument for a minimum flow velocity in the jet could be made if it were assumed that the spectral evolution of the jet is dominated by synchrotron losses rather than by particle reacceleration or by diffusion. With these assumptions, the observed spectral index of the jet would imply that the synchrotron loss bend is at a frequency above 5 GHz, so that with the equipartition assumptions made above, the particle lifetime would be $<6 \times 10^7$ yr. Combining this with the projected separation of 61 kpc between the farther component of the jet and the radio core would yield a lower limit to the bulk flow velocity of ~1000 km/s. There is strong evidence, however, for particle reacceleration in the northern jet of 3C31 from the slowness of the variation of its brightness with distance from the radio core (Burch 1979b and Paper III). The assumption that the spectrum of the jet would be dominated by synchrotron losses must therefore be regarded as dubious (see also the discussion in Sec. VI below).

V. THE BRIGHT COMPACT STRUCTURE IN THE LOBES

Figure 3(a) shows the λ6 cm map of the bright knot in the south-preceding lobe also at 0.85 × 1.2 arcsec (FWHM, major axis at p.a. = 147°) resolution. The structure is not fully resolved but can be seen to consist of two emission ridges which differ in position angle by ~110°. Most of the bright emission is contained in a region ~7 arcsec (18 kpc) across, which subtends an angle of 5.″3 at the radio core. Figure 3(b) shows the distribution of linear polarization over this region; the lengths of the vectors are proportional to the polarized intensity, and their orientations denote the position an-

TABLE IV. Flux densities and spectra of jet components.

	Following	Preceding
λ20 cm	40 ± 3 mJy	100 ± 7 mJy
λ6 cm	18 ± 2 mJy	42 ± 2 mJy
α	0.67 ± 0.12	0.73 ± 0.08

© American Astronomical Society • Provided by the NASA Astrophysics Data System

1980AJ.....85..499P

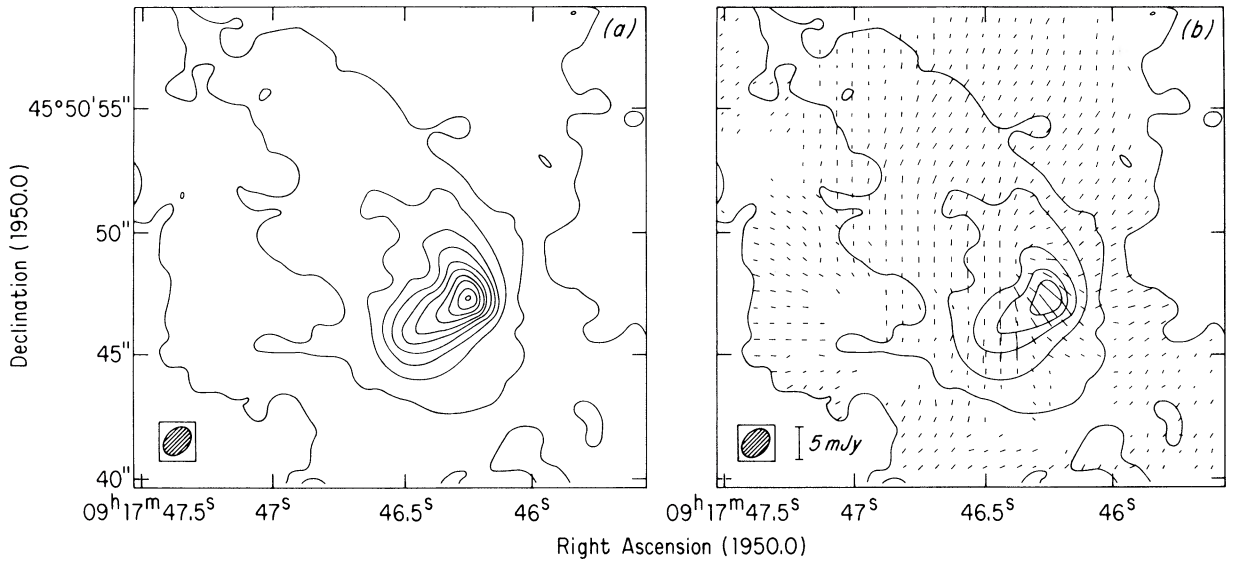

FIG. 3. (a) Contour map of total intensity in the south-preceding radio lobe of 3C219 at λ6 cm. The contour levels are 0.8, 2, 4, 6, 8, 10, 12, 14, 16, 18, and 20 mJy/beam. The full width half-power beam (0.85 arcsec × 1.2 arcsec, major axis at p.a. 147°) is indicated by the hatched ellipse at lower left. (b) The distribution of linear polarization over the south-preceding radio lobe of 3C219 at λ6 cm. The lengths of the line segments indicate the polarized intensities, and their orientations indicate the position angles of the *E* vectors. Resolution is as in (a).

gles of the *E* vectors in the received radiation. The dominant magnetic field component in this region is aligned along the brightness ridges, if the mean rotation measure of 3C219 applies at this part of the lobe.

The degree of linear polarization is typically 10–20% along the ridge of maximum brightness, and reaches a peak of 26% at the peak of total intensity. The diffuse region which surrounds the bright feature is 30–50% polarized, and the magnetic field generally envelops the bright feature.

The fine structure of the bright knot in the north-following lobe is strikingly different. Figure 4(a) shows

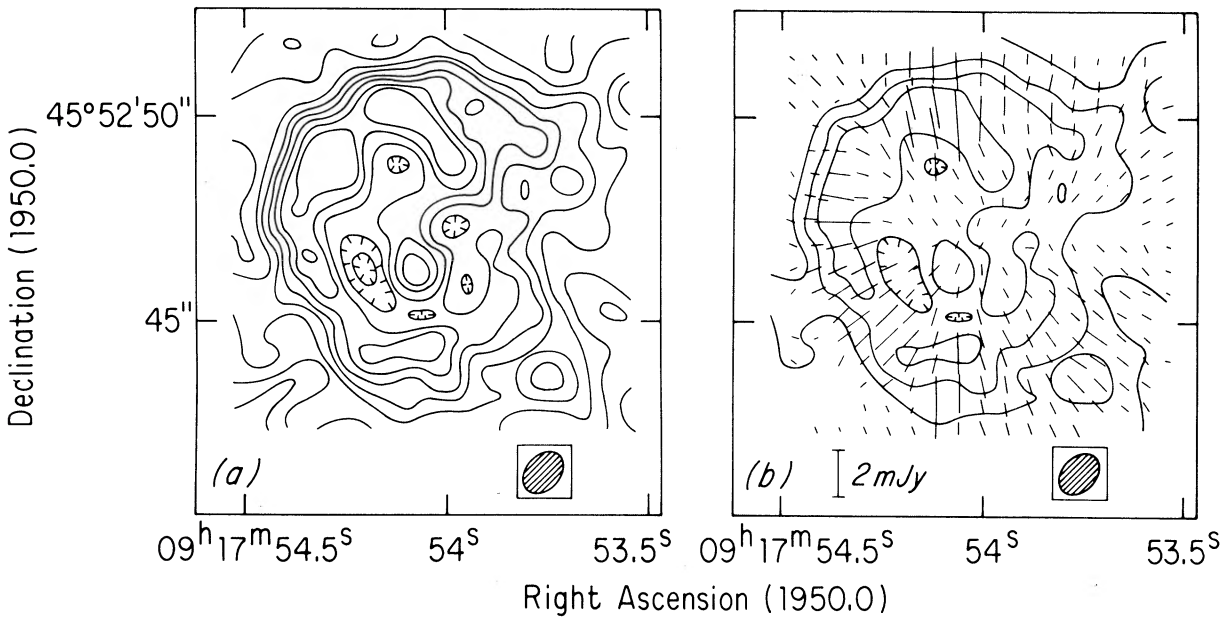

FIG. 4. (a) Contour maps of detail in the brightest feature in the north-preceding lobe of 3C219 at λ6 cm. The contour levels are 0.4, 0.8, 1.2, 1.6, 2.0, 2.5, 2.9, 3.3, and 3.7 mJy/beam. The resolution is as in Fig. 3(a), but note the changes in contour levels and in angular scale. (b) The distribution of linear polarization over the brightest feature in the north-following radio lobe of 3C219 at λ6 cm. The lengths of the line segments indicate the polarized intensities, and their orientations indicate the position angles of the *E* vectors. Resolution is as in (a).

© American Astronomical Society • Provided by the NASA Astrophysics Data System

1980AJ.....85..499P

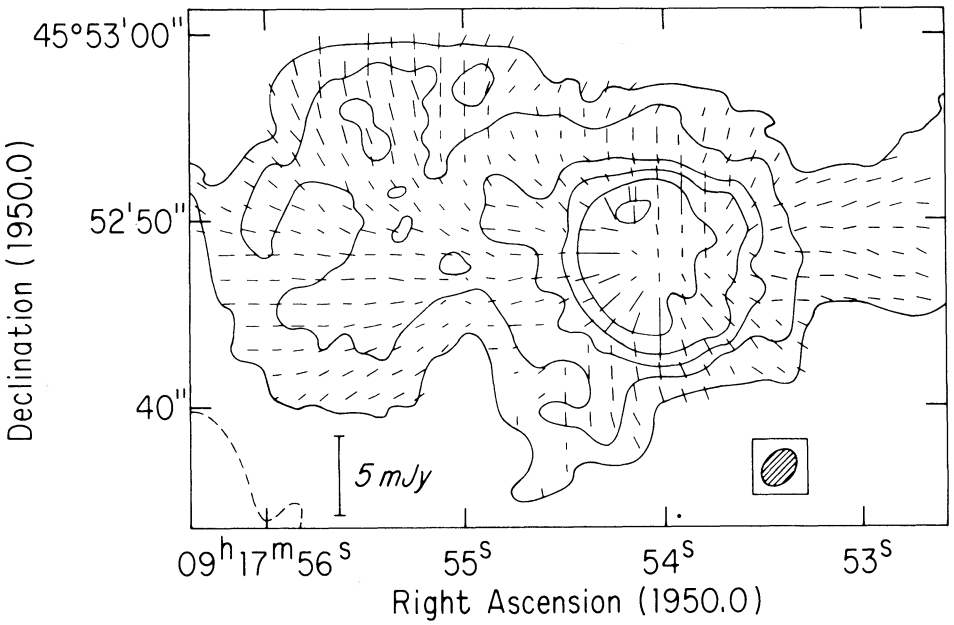

FIG. 5. The distribution of linear polarization over the entire north-following lobe of 3C219 at λ6 cm. The total intensity contours are 0.95, 1.9, 2.8, 3.8, 5.7, and 9.5 mJy/beam. The lengths of the line segments indicate the polarized intensities, and their orientations indicate the position angles of the *E* vectors. The full width half-power beam (1.4 arcsec × 1.8 arcsec, major axis at p.a. 133°) is indicated by the hatched ellipse at lower right.

the λ6 cm map of this region at the same resolution as Fig. 3(a). The feature has a nearly complete ring structure, strikingly reminiscent of a galactic supernova remnant were it not for its linear scale: the diameter of the ring is ~7 arcsec (18 kpc) at the distance of 3C219. The probability that an actual galactic supernova remnant is superimposed on the maximum of the diffuse emission of the northern lobe, at b^{II} ~45°, is negligible. Not one of the 130 galactic radio supernova remnants in the all-sky catalog of Clark and Caswell (1976) is farther than 10° from the galactic plane.

The *E* vectors in the ring [Fig. 4(b)] point radially away from its center, so the magnetic field must be predominantly circumferential around the bright rim if the mean rotation measure applies here also. A similar, though larger (diameter ~30 kpc) ringlike feature with a circumferential magnetic structure can be seen in the south-preceding lobe of 3C382 (Strom *et al.* 1978; Burch 1979a), and a similar field structure is found in the north-following lobe of DA240 (Strom and Willis 1980).

The circumferential magnetic field configuration is found not only in the rim of the compact ring structure, but also in the diffuse emission surrounding the ring (Fig. 5), as was originally discovered by Fomalont (1972) and which is visible in the maps of Burch (1979a), Högbom (1979), and De Young *et al.* (1979). The degree of polarization again reaches very high values, but its variation over this lobe is not simply related to that of the total intensity. At the center of the ring, the degree of polarization is less than 3%; it increases towards the rim, reaching 20–30% there, then continues to increase up to 60% in the diffuse emission beyond the rim, i.e., the rim itself would not be discernible on a map of the degree of polarization.

VI. DISCUSSION

3C219 is between two hundred and four hundred times more luminous between 10 MHz and 10 GHz than NGC 315, 3C449, or 3C31, whose jets were studied in Papers I, II, and III. Its jet structure differs from those in these less luminous radio galaxies in several significant respects.

First, the high-brightness jet in 3C219 is one-sided and cannot be traced continuously to the southern lobe of the source. In 3C449 and 3C31 both jets extend over the entire length from the central core to the lobes (after the initial gaps near the cores are crossed), while in NGC 315 the brighter jet extends continuously from the core to its lobe and the fainter counter-jet is detected in at least three well separated locations along the path from the radio core to its lobe.

Second, the jet in 3C219 is better collimated than those in NGC 315 and 3C449 at similar distances from their radio cores (the jets in 3C31 deflect and merge into lobe structure before reaching the length of the jet in 3C219). The low-luminosity jets diverge, while the jet in 3C219 actually converges towards the edge farthest from the core, much as expected in the "independent plasmon" model (Christiansen 1971, 1973; Christiansen *et al.* 1977). If the sizes of the compact radio structures in the lobes of 3C219 are used to indicate the transverse scale of a beam associated with the jet as it enters the lobes, the hypothetical beam would have a cone angle of only ~5° when ~190 kpc from the radio core.

Third, the magnetic field in the 3C219 jet is predominantly parallel to the length of the jet for a greater distance from the radio core than it is in the jets of NGC 315 or 3C31 (Paper III) or in 3C449 (Paper II), while no indication of a transition to a perpendicular field is

© American Astronomical Society • Provided by the NASA Astrophysics Data System

1980AJ.....85..499P

detected. As the farther component of the jet is brighter than the nearer, the jet in 3C219, in a sense, brightens with increasing distance from the core for the first ~45 kpc of its length. A similar combination of increasing intensity and parallel magnetic field occurs in the first few kpc of the brighter jets in NGC 315 and 3C31 (Paper III). Furthermore, the parallel-field regimes are seen on only one side of the radio cores in these sources, an asymmetry that is also present in 3C219. In Paper III we interpreted the increasing-intensity, parallel-field regimes in NGC 315 and 3C31 as the result of stretching of magnetic-field lines that are frozen into an accelerated particle flow at the bases of these jets, and suggested that their one-sided appearance might be due to Doppler enhancement resulting from bulk relativistic motions in the proposed flows. If this interpretation applied to the entire luminous length of the jet in 3C219, it would mean that the accelerated flow maintains relativistic bulk velocities over greater distances from the radio core in 3C219 than it does in the less luminous radio galaxies. If a counter-jet is present, but is not visible owing to relativistic flow velocities (Shklovskii 1978), the quantity $\beta \cos\phi$ must exceed ~0.4, where $\beta = v/c$, v is the flow velocity, and ϕ is the angle between the flow and the line of sight.

Finally, there is a pronounced difference between the energetics of the jet in 3C219 and those of the low-luminosity radio galaxies. The jet in 3C219 has roughly 10 times the emissivity of the jets in 3C449 and transports probably 100 times the energy. When all these differences are considered, the question arises: Is the mechanism which transports particles from the core of 3C219 to its lobes the same as that operating in such low-luminosity galaxies as 3C449?

Some features of 3C219 may be easier to explain using the "independent plasmon" model of particle transport (Christiansen *et al.* 1977) than the continuous-beam models (Blandford and Rees 1974, 1978) which appear favored by the observations of the continuous low-luminosity radio jets. The blobby and abbreviated appearance of the jet in 3C219 would be naturally accounted for if the jet were emission from a group of plasmons, recently ejected from the core towards the south-preceding lobe. As such plasmons would probably not travel at bulk relativistic velocities, the absence of similar features on the other side of the source would then have to be attributed to one-sided and intermittent activity in the core. On this model the diffuse low-brightness emission around the bright radio knots could be the expanded relics of plasmons that were ejected from the core in the past, while the knots themselves would be interpreted as fresher ejecta that are now colliding with the fields and particles in these relics. In such a model the outer boundary of the relics would still be expanding outward into a circumgalactic medium and the compression of the leading edge of the relics would account for the brightness gradients observed at the extreme ends of the source structure. The setback of the bright knots into the lobes would be a natural consequence of interpreting the knots as late-arriving ejecta in the process of initial compression as they begin to interact with the relics. The diffuse bridges of emission back towards the galaxy might be accounted for by back-diffusion of relativistic particles and fields away from the compressed regions at the outer edges of the lobes.

In continuous-beam models the most important observation to explain is the sudden disappearance of the jet. If the relativistic particles were assumed not to be present beyond ~50 kpc from the core of 3C219 because a previously established beam had pinched off and was now being reestablished, the resulting "beam" description might be only semantically distinct from the "plasmon" description. If the relativistic particles in the beam instead were assumed to have been cooled by radiative losses in the first 50 kpc of the 3C219 jet, it would be difficult to explain why both of the main components of the jet have the same spectral index between λ20 cm and λ6 cm, for the electrons radiating at λ20 cm should lose energy more slowly than those radiating at λ6 cm. The most attractive interpretation of 3C219 in a continuous-beam model may therefore be to suppose that the radiative losses from a beam in 3C219 sharply decrease ~50 kpc from the core owing to narrowing of the pitch-angle distribution of the relativistic particles around the magnetic field lines in the beam. Streaming of the particle motions along the field lines would cause each particle to radiate less energy and the beam's radiation to become less directed towards the observer. As the degrees of polarization found in all of the radio jets so far indicate that they do contain well organized magnetic field configurations, the directive properties of synchrotron radiation from a highly organized beam may be the most plausible way to make a very efficient and invisible beam supply energy to the lobes of the very luminous sources in which no radio jets have yet been detected.

The continuous-beam models do not provide a simple explanation for the very different detailed configurations seen within the two bright knots in the lobes of 3C219, or for the distributions of the low-brightness emission around them. Beams of particles and fields would be compressed on reaching the turbulent "working surface" proposed by Blandford and Rees (1974). The field components $B_\perp$ perpendicular to the beam should be amplified there and the relativistic particles in the beams would travel at large pitch angles to these suddenly compressed fields. A brightening of the radiation from the beam, and a perpendicular field structure are therefore likely characteristics of a region where the beam is about to terminate and deposit its particles in the lobes. Freezing of the magnetic fields into a particle flow that stretched them predominantly away from the deposition region would then produce L- and U-shaped field configurations at bright parts of the lobes. Such a scenario may be able to explain the observed brightness and polarization distributions in the south-preceding lobe

© American Astronomical Society • Provided by the NASA Astrophysics Data System

1980AJ.....85..499P

of 3C219. The shell structure seen in the total intensity distribution of the knot in the north-following lobe, and the associated circumferential magnetic field configuration are less easy to explain.

The structure of the low-brightness emission between the core and the two bright knots in the lobes resembles that suggested by Scheuer (1974) to act as a depository for waste energy that would necessarily be transported to the lobes by beams of particles and fields. The asymmetry in the distribution of this emission between the lobes themselves is puzzling, however.

The relationship of the jet in 3C219 to those in less luminous radio galaxies, which fit readily into the predictions of continuous-beam models, therefore remains enigmatic. A search for other high-luminosity jets in radio galaxies and quasars is now in progress at the VLA to test whether the many peculiarities of 3C219 are unique to this source or whether they are representative of more general behavior at higher radio luminosities.

We thank the staff of the VLA for its support of these observations. This work was partially supported by an operating grant to A.H.B. from the Natural Sciences and Engineering Research Council of Canada and by National Science Foundation grant AST 77-22906 to A.G.W. while he was at Brandeis University.

REFERENCES

Baars, J. W. M., Genzel, R., Pauliny-Toth, I. I. K., and Witzel, A. (1977). Astron. Astrophys. Suppl. **61,** 99.
Blandford, R. D., and Rees, M. J. (1974). Mon. Not. R. Astron. Soc. **169,** 395.
Blandford, R. D., and Rees, M. J. (1978). Phys. Scr. **17,** 265.
Bridle, A. H., Davis, M. M., Fomalont, E. B., Willis, A. G., and Strom, R. G. (1979). Astrophys. J. **228,** L9 (Paper I).
Burch, S. F. (1979a). Mon. Not. R. Astron. Soc. **186,** 519.
Burch, S. F. (1979b). Mon. Not. R. Astron. Soc. **187,** 187.
Christiansen, W. A. (1971). Astrophys. Lett. **1,** 233.
Christiansen, W. A. (1973). Mon. Not. R. Astron. Soc. **164,** 211.
Christiansen, W. A., Pacholczyk, A. G., and Scott, J. S. (1977). Nature **266,** 593.
Clark, D. H., and Caswell, J. L. (1976). Mon. Not. R. Astron. Soc. **174,** 267.
De Young, D. S., Hogg, D. E., and Wilkes, C. T. (1979). Astrophys. J. **228,** 43.
Fomalont, E. B. (1972). Astrophys. Lett. **12,** 187.
Fomalont, E. B., Bridle, A. H., Willis, A. G., and Perley , R. A. (1980). Astrophys. J. (in press) (Paper III).
Högbom, J. A. (1974). Astron. Astrophys. Suppl. **15,** 417.
Högbom, J. A. (1979). Astron. Astrophys. Suppl. **36,** 173.
Macdonald, G. H., Kenderdine, S., and Neville, A. C. (1968). Mon. Not. R. Astron. Soc. **133,** 251.
Perley, R. A., Willis, A. G., and Scott, J. S. (1979). Nature **281,** 437 (Paper II).
Scheuer, P. A. G. (1974). Mon. Not. R. Astron. Soc. **166,** 513.
Schmidt, M. (1965). Astrophys. J. **141,** 1.
Shklovskii, I. S. (1978). Sov. Astron. **21,** 401.
Strom, R. G., and Willis, A. G. (1980). In preparation.
Strom, R. G., Willis, A. G., and Wilson, A. S. (1978). Astron. Astrophys. **68,** 367.
Turland, B. D. (1975). Mon. Not. R. Astron. Soc. **172,** 181.
Willis, A. G., Strom, R. G., and Wilson, A. S. (1974). Nature **250,** 625.

© American Astronomical Society • Provided by the NASA Astrophysics Data System